Activity Profiling in Catalytic Reactors

Profiling the activity can decrease sensitivity to temperature runaway when incomplete reaction is avoided in the less active front zone.

Carl Pirkle, Jr. and Israel E. Wachs, Exxon Research and Engineering Co., Annandale, NJ 08801

The possibility of temperature runaway is a major concern in the operation of nonadiabatic, catalytic tubular reactors. To prevent this problem, reaction engineers have advocated the profiling of catalytic activity the reactor so that a less active catalyst is located where chemical potential driving force is greatest *(6-8)*. For *n*th reactions $(n > 0)$, this requires a less active catalyst the front portion of the reactor. Earlier computer simulations of activity-profiled reactors demonstrate a reduction parametric sensitivity to temperature runaway compared uniform-activity reactors with the same conversion and activity *(9-11)*. Simulations of this sort are commonly presented in textbooks on reactor engineering.

Sensitivity reversal can occur in the face of certain upsets during the operation of activity-profiled reactors, such as activation of the catalyst in the inlet zone of the reactor the incomplete preheating of reactant feed. Sensitivity reversal means that the reactor becomes more sensitive to temperature runaway when the upsets occur, rather than sensitive as might be expected. The reaction system for the simulation of this sensitivity reversal is the par-

tial oxidation of orthoxylene to form phthalic anhydride. The kinetic model chosen to describe this reaction is a simple mechanism proposed by Froment *(12)*. Froment's mechanism was chosen simply because it has been used on several occasions to demonstrate the reduced sensitivity of activity-profiled reactors to temperature runaway *(9,13,14)*.

Mathematical model

Nonadiabatic fixed-bed reactor systems at steady state can be described by a set of partial differential equations corresponding to continuity of mass and energy as well as pressure drop. A variety of models were classified by Froment *(15)*, Table 1.

For highly exothermic reactions, significant temperature gradients exist across the reactor tube radius, requiring models with two spatial variables (the axial and radial posi-

Carl Pirkle, *a research associate in the Corporate Research Laboratories of Exxon Research and Engineering Co., is involved in mathematical modeling. After receiving degrees in chemical engineering the Georgia Institute of Technology (B.Ch.E., M.S., Ph.D.), he the Johns Hopkins Applied Physics Laboratory, where he performed theoretical research in chemical lasers. Before joining Exxon, as on the faculty of the Johns Hopkins Univ. School of Medicine where he conducted research in biomedical engineering.*

Israel Wachs *received his chemical engineering degrees from the City College of the City Univ. of New York (B.E.) and Stanford University and Ph.D.). He has been employed by the Corporate Research Laboratories since graduation from Stanford. In January 1987, he joined the faculty of the Dept. of Chemical Engineering at Lehigh. His interests are in fundamental and applied research for heterogeneous catalysis.*

Table 1. Steady-state models for fixed-bed tubular reactors.

Model	Space Dimension	Flow Pattern	Treatment of Phases
A.I	Axial	Plug flow	Pseudohomogeneous
A.II	Axial	Axial dispersion	Pseudohomogeneous
A.III	Axial Radial (tube)	Radial dispersion	Pseudohomogeneous
B.I	Axial	Plug flow	Interfacial gradients
B.II	Axial Radial (pellet)	Plug flow	Interfacial and intrapellet gradients
B.III	Axial Radial (tube)	Radial dispersion/ Radial velocity profile (optional)	Interfacial gradients

tion of a typical reactor tube) for accurate simulation. The A.III model in Table 1 assumes plug flow of gas and provides for radial dispersion of heat and mass but neglects heat transfer resistance between the gas and catalyst phases. This is called the pseudohomogeneous treatment and results in a single energy equation and temperature for both phases. The more comprehensive B.III model includes a separate energy equation (and temperature) for each of the two phases coupled by terms for interphase transfer of heat. In both the A.III and B.III models, axial dispersion of heat and mass are neglected, a valid assumption for most commercial reactors (16).
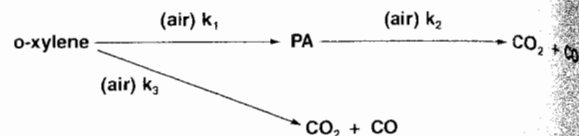
In the set of simulations presented here, Froment's A.III model is used along with the assumption of negligible pressure drop. For kinetic rates, his simple model for phthalic anhydride synthesis from orthoxylene, Figure 1, is adopted (12). This allows comparison of previous studies of activity-profiled reactors with results designed to demonstrate the effect of certain upsets on parametric sensitivity, e.g., catalyst deactivation or incomplete heating of the reactant feed. Extensive calculations were made using the more comprehensive B.III model that includes interphase transfer of heat and mass. Predictions for sensitivity reversal obtained by the more elaborate model are qualitatively similar to those obtained by the A.III model, whose results are presented in this article.

Simulations with A.III model

In the simulations performed with the A.III model, the parameters in Table 2 were used to study the parametric sensitivity of the phthalic anhydride reactor both with and

$$R_1 = k_1 p_{ox} p_o \ ; \ \ln k_1 = \frac{-13588}{T} + 11.597$$

$$R_2 = k_2 p_{PA} p_o \ ; \ \ln k_2 = \frac{-15601}{T} + 12.619$$

$$R_3 = k_3 P_{ox} P_o \ ; \ \ln k_3 = \frac{-14394}{T} + 10.730$$

$$\Delta H_1 = -1{,}294{,}000 \text{ kJ/kmol}, \quad \Delta H_3 = -4{,}564{,}000 \text{ kJ/kmol}$$

Figure 1. Kinetic mechanism for partial oxidation of O-xylene over V_2O_5 to form phthalic anhydride.

without activity profiling. The partial differential equations and associated boundary conditions comprising the A.III model are presented elsewhere (14,15). As in the case of previous studies (9,12-16), pressure drop and temperature dependence of all thermophysical properties (except for density of the gas phase) were neglected. The pressure drop is calculated to be about 0.05 MPa for the flow conditions, bed length, and particle size used in Table 2, which is significant. However, an actual commercial reactor will have a lower pressure drop, so the neglect of pressure variation in the model may introduce only a second-order error in simulation.

It has been demonstrated that the solutions of the system of partial differential equations comprising model A.III or B.III can be conveniently obtained from either of two general software packages, PDECOL or DSS/2 (17). Both of these packages use a numerical method of lines approach, in which the radial dimension of the tubular reactor is discretized, resulting in a system of ordinary differential equations with respect to the axial position z. The ODE system is usually stiff and should be integrated by implicit techniques developed for such systems. For the spatial discretization in the radial dimension, PDECOL uses B-spline basis functions (18), and DSS/2 has been modified recently to allow use of either a variety of finite difference methods or orthogonal collocation on finite elements (19). Both the PDECOL and modified DSS/2 packages have excellent stiff integration routines. Solutions can be obtained accurately and efficiently, requiring about 10 CPU (central processing unit) seconds per run on an IBM 3033.

In addition to PDECOL or DSS/2, other general purpose partial differential equations solvers are available, whose list was included in a recent review (20). Many of these packages provide the power to solve a wide variety of partial differential equation systems but require only a modest amount of numerical training of the user.

Activity profiling in normal operation

For a uniform catalyst-bed activity, Table 3 shows the conversion of orthoxylene, selectivity to phthalic anhydride, maximum temperature and its location in the reactor for

Table 2. Parameters used in A.III Model of phthalic anhydride synthesis reactor.

Operating Condition	Value
Inlet Temp., T_o	630 to 720 K
Inlet Pres., P_o	0.1014 MPa
Mass Flux of Air, G_s	1.2579 kg/m²·s
Inlet Conc. of O-Xylene, w_{10}	0.31343×10^{-3} kmol/kg
Gas-Phase Spec. Heat, C_{pt}	1.059 kJ/kg·K
Tube Dia. (Inside), d_t	0.0250 m
Tube Length, L	3.75 m
Catalyst Bulk Density, ρ_B	1,300 kg/m³
Interparticle Bed Voidage, ε	0.38
Pellet Dia., d_p	0.003 m
Effective Thermal Cond., λ_{er}	2.051×10^{-3} kJ/m·s·K
Wall Heat Transfer Coeff., h_w	0.1558 kJ/m²·s·K
Radial Peclet No. for Mass, Pe_M	10.0

The possibility of temperature runaway is a major concern the operation of nonadiabatic, catalytic tubular reactors.

(air) k_2 → CO_2

$CO_2 + CO$

; $\ln k_1 = \dfrac{-13588}{T} + 11.597$

; $\ln k_2 = \dfrac{-15601}{T} + 12.619$

; $\ln k_3 = \dfrac{-14394}{T} + 10.730$

/kmol, $\Delta H_3 = -4{,}564{,}000$ kJ/kmol

nism for partial oxidation of O-xylene... ydride.

ing. The partial differential equ...
dary conditions comprising the...
elsewhere (14,15). As in the c...
?-16), pressure drop and temper...
iermophysical properties (exce...
se) were neglected. The pressure...
out 0.05 MPa for the flow cond...
cle size used in Table 2, which...
actual commercial reactor will...
so the neglect of pressure variat...
uce only a second-order error i...

trated that the solutions of the s...
equations comprising model A...
ntly obtained from either of two...
es, PDECOL or DSS/2 (17). B...
numerical method of lines app...
mension of the tubular reactor...
a system of ordinary differential...
he axial position z. The ODE s...
iould be integrated by implicit...
such systems. For the spatial di...
nension, PDECOL uses B-spline...
SS/2 has been modified recently...
iriety of finite difference meth...
n on finite elements (19). Bo...
d DSS/2 packages have excelle...
Solutions can be obtained acc...
ng about 10 CPU (central proc...
on an IBM 3033.
:OL or DSS/2, other general pu...
ations solvers are available, wh...
ent review (20). Many of these...
to solve a wide variety of part...
ms but require only a modest a...
of the user.

in normal operation

yst-bed activity, Table 3 sho...
ne, selectivity to phthalic anh...
and its location in the react...

Table 3. Effect of inlet temperature and reactant concentration on performance of reactor with uniform catalyst activity.

w_{10}, kmol/kg	T_{max}, K	z_{max}, m	Selectivity	Conversion
0.00031343	672.1	0.50	0.7991	0.8053
0.00031343	692.7	0.56	0.7776	0.8504
0.00031343	700.9	0.63	0.7690	0.8640
	Temperature Runaway		0.0000	1.0000
0.00032000	675.7	0.50	0.7970	0.8099
0.00033000	683.7	0.56	0.7924	0.8196
0.00034000	700.0	0.63	0.7807	0.8409
0.00034250	711.0	0.69	0.7707	0.8563
0.00034500	Temperature Runaway		0.0000	1.0000

...rent inlet temperatures T_0 and orthoxylene concentra-...s w_{10}. In these calculations coolant temperature T_C is set ...al to the inlet temperature T_0. Here, T_{max} is the maxi-...m temperature within the reactor, and z_{max} is the axial ...tion corresponding to T_{max}, reported within $\pm$ 0.05 m. ...radial position for T_{max} is always the tube center. ...the minimum acceptable levels of conversion of orthox-...re are set at 80% and selectivity to phthalic anhydride at

Table 4. Effect of inlet and coolant temperatures on performance of reactor with programmed catalyst activity: $F_1 = 0.66667$; $F_2 = 1.00$; $z_1 = 0.75$ m.

T_c	w_{10} kmol/kg	T_{max} K	z_{max} m	Selectivity	Conversion
	0.00031343	663.2	1.13	0.7979	0.8058
	0.00031343	668.7	1.06	0.7868	0.8318
	0.00031343	676.7	1.06	0.7688	0.8659
	0.00031343	681.5	1.06	0.7557	0.8860
	0.00031343	687.9	1.06	0.7398	0.9059
	0.00031343	692.0	1.00	0.7236	0.9225
	0.00031343	709.8	0.56	0.7023	0.9392
	0.00031343	740.8	0.94	0.6420	0.9662
		Temperature Runaway		0.0000	1.0000
	0.00035000	672.8	1.13	0.7911	0.8205
	0.00038000	684.7	1.19	0.7828	0.8363
	0.00039000	693.2	1.19	0.7764	0.8471
	0.00040000	717.4	1.31	0.7530	0.8794
	0.00040250	Temperature Runaway		0.0000	1.0000

70%, there is only a narrow range of inlet temperatures and reactant concentrations for acceptable operation. Temperature runaway can occur for inlet temperatures that are too high for a given inlet reactant concentration or vice versa.

As case studies, some textbooks (13,16) examine the effect of activity profiling on the operability of a phthalic anhydride reactor system with parameters similar to those in Table 2. Profiling can be accomplished either by varying the number of active sites within each catalyst pellet or by diluting the catalyst bed with inert pellets.

The simulations presented here use a form of activity profiling examined previously (13,14). Mathematically, the activity profiling is represented by an activity factor F that multiplies the rate constants k_1, k_2, and k_3 given in Figure 1. The factor F is a function of axial position z in a typical reactor tube

$$F = F_1, \; 0 < z < z_1 \qquad (1)$$
$$F = F_2, \; z > z_1$$

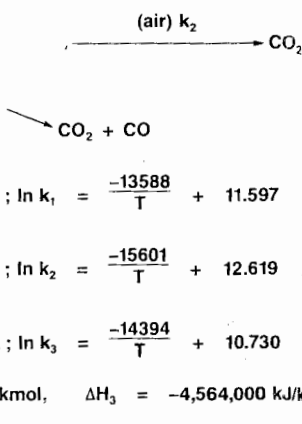Using $F_1 = 0.66667$, $F_2 = 1.00$, $z_1 = 0.75$ m, and $T_C = T_0$, the results in Table 4 are obtained.

For the activity-profiled reactor, $T_0 = T_C = 633$ K results in the same selectivity and conversion as $T_0 = T_C = 630$ K in the reactor with uniform activity, Table 3, when $w_{10} = 0.00031343$ kmol/kg. It is also obvious that the activity-profiled reactor allows a wider range of $T_0 = T_C$ values before temperature runaway occurs (14.0 vs. 3.5 K).

Similarly, if the lower parts of Tables 3 and 4 are compared, it is clear that the activity-profiled reactor allows higher values of the inlet reactant concentration over that of the uniform-activity reactor (0.00040 vs. 0.00034 kmol/kg). Both of these advantages are further illustrated by comparing the centerline temperature profiles given in Figures 2 to 5.

The effect of inlet reactant concentration for values of $T_0 = T_C$ greater than 633 K was also investigated. As inlet and coolant temperature increase, the value of the inlet concentration leading to temperature runaway decreases. For $T_0 = T_C = 638$, 640 or 642 K, temperature runaway occurs if $w_{10} > 0.0003725$, 0.0003600 or 0.0003475 kmol/kg, respectively.

Activity profiling in abnormal operation

It can be concluded that reduction of activity in the front part of the reactor increases operability with respect to variations in coolant temperature and/or reactant loading by decreasing parametric sensitivity to temperature runaway. This is true as long as the activity-profiled reactor operates as designed. However, there are various potential upsets in the reactor operation that can actually increase parametric
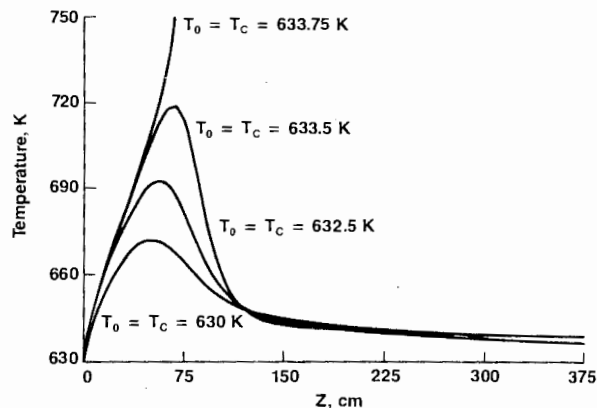
Figure 2. Centerline temperature profiles for uniform catalytic activity vs. inlet/coolant temperature: $F_1 = F_2 = 1.0$; $w_{10} = 0.00031343$ kmol/kg·s.
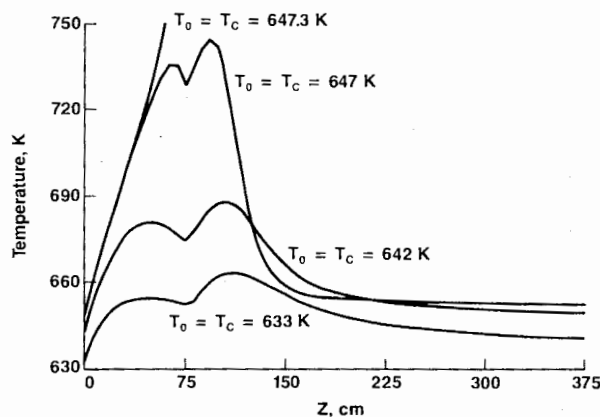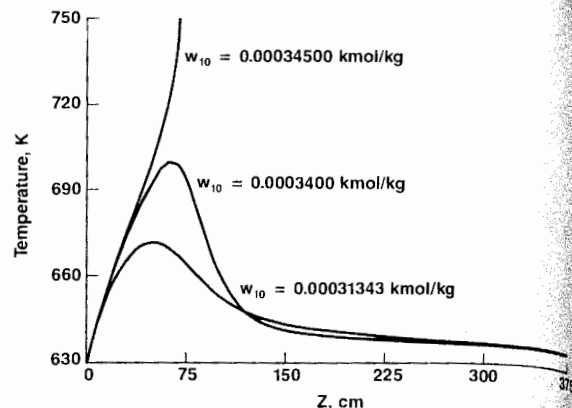

Figure 3. Centerline temperature profiles for uniform catalytic activity vs. inlet O-xylene concentration: $F_1 = F_2 = 1.0$; $T_0 = T_C = 630$ K.
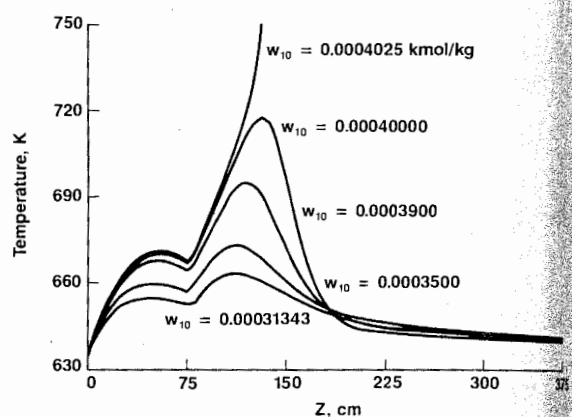

Figure 4. Centerline temperature profiles for profiled-catalytic activity vs. inlet/coolant temperature: $F_1 = 0.66667$, $F_2 = 1.0$, $z_1 = 0.075$ m; $w_{10} = 0.00031343$ kmol/kg·s.

Figure 5. Centerline temperature profiles for profiled-catalytic activity vs. inlet concentration of O-xylene: $F_1 = 0.66667$, $F_2 = 1.0$, $z_1 = 0.075$ m; $T_0 = T_C = 633$ K.

sensitivity to temperature runaway. Among these are the deactivation of catalyst near the reactor inlet by a contaminant in the reactants or by a locally excessive temperature, which slowly sinters the catalyst. Another possible upset is the incomplete preheating of the reactant mixture before it reaches the catalyst, i.e., T_0 lies below its design value.

Table 5 shows the effect of variation in catalytic activity in the front portion of the reactor for $T_0 = T_C = 640$ K,

$w_{10} = 0.00031343$ kmol/kg, and $F_2 = 1.0$. As the fractional activity F_1 in the reactor bed inlet decreases below the design value of 0.66667, the maximum temperature and conversion increase and the selectivity decreases. On the other hand, the maximum temperature and conversion also increase and the selectivity decreases as F_1 takes on higher values than 0.66667. Thus, there is clearly a value of F_1 that minimizes T_{max} for given values of $T_0 = T_C$, F_2, z_1, and w_{10}. As a result, a window of values exists for F_1 (0.45 to 0.80) which results in acceptable levels of conversion and selectivity and does not cause temperature runaway. Additional calculations indicate that the width of this window decreases as $T_0 = T_C$ increases. For $T_0 = T_C = 638$ and 642 K, the window in F_1 is 0.35 to 0.85 and 0.525 to 0.775, respectively.

The effect of inlet temperature T_0 on the performance of the activity-profiled reactor is given in Table 6 for $T_C = 640$ K, $F_1 = 0.66667$, $z_1 = 0.75$ m, $F_2 = 1.0$, and $w_{10} = 0.00031343$ kmol/kg. Here, it is apparent that the tendency for temperature runaway to occur increases as inlet temperature declines, the opposite of what might be expected intuitively from experience with reactors possessing uniform

/kg

3400 kmol/kg

0.00031343 kmol/kg

0	225	300

Z, cm

e profiles for uniform catalytic acti
ion: F₁=F₂=1.0; T₀ = T_C = 630 K

₀ = 0.0004025 kmol/kg

w₁₀ = 0.00040000

w₁₀ = 0.0003900

w₁₀ = 0.0003500

₁343

150	225	300

Z, cm

ıre profiles for profiled-catalytic ad
-xylene: F₁ = 0.66667, F₂ = 1.0,

catalytic activity. In fact, if the reactant feed enters the catalyst bed at $T_0 = 450$ K, temperature runaway ensues. Additional calculations show that for coolant temperatures $T_C = 638$ and 642 K, inlet temperatures T_0 less than 300 and 575 K, respectively, will lead to temperature runaway. Thus, the greater the value of the coolant temperature, the more serious the problem of incomplete preheating becomes.

The phenomena reported in Tables 5 and 6 for reactors with activity profiling according to Eq. 1 can be referred to
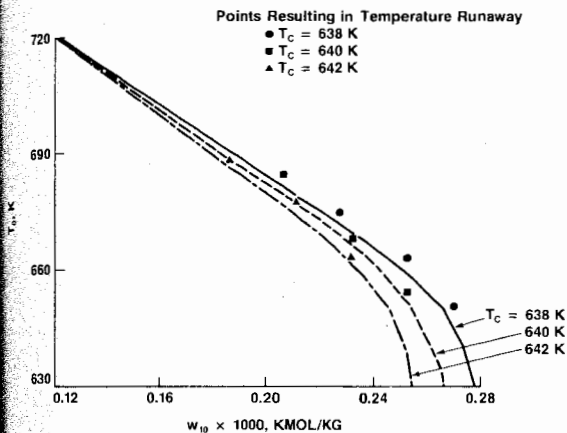

Figure 6. Sensitivity limit curves for T_C = 638, 640 and 642 K with points resulting in temperature runaway.

g, and $F_2 = 1.0$. As the fraction as "sensitivity reversal." This is because the tendency for bed inlet decreases below the these reactors to undergo temperature runaway can actually increase as T_0 and F_1 decline rather than monotonically decreasing as is always the case in a uniformly active bed.

This reverse sensitivity to F_1 and T_0 for activity-profiled reactors can be explained by the use of sensitivity limit curves generated for the case of uniform activity ($F = 1.0$ for $0 < z < L$) and various values of the coolant temperature. Sensitivity limit curves are defined as plots in the T_0, w_{10} plane such that any reactant mixture entering a fully active catalyst zone with a temperature and reactant concentration lying above the curve will experience temperature runaway. Figure 6 gives the sensitivity limit curves for the cases $T_C = 638$, 640 and 642 K. Because we are dealing with a two-dimensional reactor model, the curves in Figure 6 are generated by an iterative numerical procedure rather than by the more elegant methods proposed for one-dimensional reactor models (3-5). For a given value of T_0, the value of w_{10} is found to be just sufficient to cause temperature runaway, which is defined as selectivity dropping below 0.6 for this particular reaction scheme. This defini-

tion is less conservative than one based on the appearance of a positive second derivative in the centerline temperature vs. orthoxylene conversion plane (4).

In the case of activity-profiled reactors, if the pair of values, $y_{1,1}$ and T_1 (the concentration and temperature at the entrance z_1 of the most active region of the catalyst bed), correspond to points lying above the sensitivity limit curves, temperature runaway occurs. Otherwise, the reaction proceeds without temperature runaway. The points plotted in Figure 6 correspond to some values of T_1 and $y_{1,1}$ that just lead to runaway for the indicated values of T_C. It is obvious that these points lie above their respective sensitivity limit curves, thus correctly predicting that temperature runaway should occur in each case.

Table 5. Effect of front-end activity on performance of reactor with activity profile: $T_0 = T_C = 640$ K; $F_2 = 1.00$; $z_1 = 0.75$ m; $w_{10} = 0.00031343$ kmol/kg.

F_1	T_{max} K	z_{max} m	Selectivity	Conversion	T_1 K	$y_{1,1}$
	Temperature					
0.825	Runaway		0.0000	1.0000	747.2	0.2600
0.80	704.1	0.56	0.7406	0.9044	692.0	0.4498
0.75	686.6	0.50	0.7516	0.8921	677.5	0.5594
0.66667	681.5	1.06	0.7557	0.8860	668.3	0.6573
0.60	687.4	1.13	0.7552	0.8856	663.5	0.7133
0.50	706.1	1.25	0.7439	0.8971	657.9	0.7806
0.45	727.3	1.38	0.7211	0.9167	655.5	0.8096
	Temperature					
0.44	Runaway		0.0000	1.0000	655.0	0.8150

Table 6. Effect of inlet temperature on performance of reactor with activity profile: $T_C = 640$ K; $F_1 = 0.66667$; $F_2 = 1.00$; $z_1 = 0.75$ m; $w_{10} = 0.00031343$ kmol/kg.

T_0 K	T_{max} K	z_{max} m	Selectivity	Conversion	T_1 K	$y_{1,1}$
640	681.5	1.06	0.7546	0.8860	668.3	0.6573
600	693.0	1.13	0.7508	0.8912	670.1	0.7040
575	700.4	1.13	0.7456	0.8966	670.6	0.7206
550	706.1	1.19	0.7413	0.9008	670.9	0.7331
525	713.1	1.19	0.7348	0.9067	670.9	0.7329
500	722.5	1.25	0.7243	0.9156	671.0	0.7510
475	754.6	1.38	0.6714	0.9472	671.0	0.7579
	Temperature					
450	Runaway		0.0000	1.0000	671.0	0.7640

Parametric sensitivity

Parametric sensitivity is pronounced in exothermic fixed-bed reactors with uniform catalytic activity. For conditions leading to acceptable selectivity and conversion, the operating windows for $T_0 = T_C$ and w_{10} are very narrow, 3.5 K and 0.00003 kmol/kg, respectively. For the activity-profiled reactor, acceptable selectivity and conversion can be obtained with wider, safe-operating windows in $T_0 = T_C$ and w_{10}, 14.0 K and 0.00006 kmol/kg, respectively. Taking advantage of these greater margins of safety, T_0 and/or w_{10} can be increased to obtain even higher production yields in the reactor. As long as the catalyst in the front part of the activity-profiled reactor maintains its design activity and the preheating of the reactant feed is adequate, the parametric sensitivity to temperature runaway should remain low.

If the catalyst activity in the front portion of the activity-profiled reactor is reduced below its design value by some contaminant in the inlet stream, temperature runaway may occur in the more active downstream section. Although this result may be surprising, it can be explained by the higher reactant concentration at z_1, the beginning of the active zone. The pair of values T_1 and $y_{1,1}$ corresponding to temperature runaway are seen to lie above the appropriate sensitivity limit curves. Thus, the front portion of the reactor is insufficiently active to reduce $y_{1,1}$ below the critical value that leads to temperature runaway.

A similar phenomenon is observed in the case of incomplete preheating of the feed. Because of the reduced temperature in the less active upstream zone of the reactor, $y_{1,1}$ and T_1 can lie above the sensitivity limit curve, and temperature runaway will occur in the more active downstream zone.

The activity profile, Eq. 1, used in this simulation and in previous studies, is rather simplified, although it appears to be effective. More optimal activity profiles have been proposed by others (9-11). However, the qualitative effect of front-zone catalyst deactivation and/or incomplete preheating of feed will still be the same. If, at some level of front-end deactivation or some degree of incomplete preheating, a pair of values T_1 and $y_{1,1}$ emerge that lie above the sensitivity limit curve, temperature runaway will occur.

Generation of the sensitivity limit curve requires repetitive numerical calculations, although a suitable optimization scheme can reduce the computational effort. More elegant procedures have been proposed for one-dimensional reactor models (3-5). At any rate, curves of the type shown in Figure 6 can be used in design studies to determine the consequences of front-end catalyst deactivation or incomplete preheating of feed on reactor sensitivity.

Profiling the activity in catalytic fixed-bed reactors can decrease sensitivity to temperature runaway, but care must be taken to avoid incomplete reaction in the less active front zone. If the feed is not sufficiently preheated, the extent of reaction in the front zone will be less than planned. If partial catalyst deactivation occurs in the front zone of the reactor, less reaction occurs before the reactant mixture reaches the more active downstream zone. If the gas-phase concentration and temperature entering the downstream zone lie above the sensitivity limit curve, temperature runaway will occur. ∎

Notation

C_{pl} = specific heat of gas phase, kcal/kg·K
d_p = diameter of catalyst pellet, m
d_i = inside diameter of reactor tube, m
F_1 = activity factor for front zone of catalyst bed
F_2 = activity factor for second, more active zone of catalyst bed
G_a = mass flux of air, kg/m²·s
h_w = heat transfer coefficient at tube wall, kJ/m²·s·K
k_j = rate constant of jth reaction, kmol/kg cat·bar²·s
L = length of catalyst bed, m
p_i = partial pressure of species i, bar
P_0 = inlet total pressure, bar
Pe_M = Peclet number for radial dispersion of mass
r = radial position in reactor tube
R_j = rate of jth reaction, kmol/m³·s
T = temperature in reactor, K
T_C = coolant temperature, K
T_a = inlet temperature of gas, K
T_{max} = maximum temperature in reactor, K
T_1 = temperature at entrance of second zone, K
w_i = gas-phase concentration of species i, kmol of i/kg of gas
w_{10} = inlet concentration of species 1 (o-xylene), kmol/kg
y_i = w_i/w_{10}
$y_{1,1}$ = dimensionless concentration of species i at entrance to second zone of reactor
z = axial position of reactor, m
z_{max} = axial position of maximum temperature in reactor, m
z_1 = axial position of entrance to second zone of reactor

Greek letters

ΔH_j = heat of reaction of jth reaction, kJ/mol
ϵ = external voidage of catalyst bed
λ_{er} = effective thermal conductivity in radial direction, kJ/m·s·K
ρ_a = bulk density of catalyst, kg/m³

Literature cited

1. Bilous, O., and N.R. Amundson, *AIChE J.*, **2**, p. 117 (1956).
2. Van Welsenaere, R.J., and G.F. Froment, *Chem. Eng. Sci.*, **25**, p. 1503 (1970).
3. Morbidelli, M., and A. Varma, *AIChE J.*, **28**, p. 705 (1982).
4. Morbidelli, M., and A. Varma, *Chem. Eng. Sci.*, **40**, p. 2165 (1985).
5. Morbidelli, M., and A. Varma, *Chem. Eng. Sci.*, **41**, p. 1063 (1986).
6. Dreyfus, H., U.S. Patent No. 2,393,240 (1946).
7. Egbert, R.B., U.S. Patent No. 2,764,598 (1956).
8. Calderbank, P.H., A. Caldwell, and G. Ross, *Chimie et Industrie-Genie Chimique*, **2**, p. 101 (1969).
9. Caldwell, A.D., and P.H. Calderbank, *Brit. Chem. Eng.*, **9**, p. 14 (1969).
10. Narsimhan, G., *Ind. Eng. Chem. Process Des. Dev.*, **15**, p. 302 (1976).
11. Sadhukhan, P., and E.E. Petersen, *AIChE J.*, **22**, p. 808 (Sept. 1976).
12. Froment, G.F., *Ind. Eng. Chem.*, **59**, p. 18 (1967).
13. Rase, H.F., "Chemical Reactor Design for Process Plants," **II**, John Wiley, New York (1977).
14. Pirkle, Jr., J.C., and I.E. Wachs, "A Reassessment of Activity Profiling in Exothermic, Fixed-Bed Catalytic Reactors," Paper No. 48f, AIChE Meeting, Miami (Nov. 2-7, 1986).
15. Froment, G.F., "Fixed-Bed Reactors—Steady State Conditions," *Proc. Eur. Symp. Chem. React. Eng.*, Elsevier, Amsterdam (1972).
16. Froment, G.F., and K.B. Bischoff, "Chemical Reactor Analysis and Design," John Wiley, New York (1979).
17. Pirkle, Jr., J.C., I.E. Wachs, and J.E. Sobel, "Foundations of Computer-Aided Process Design," **II**, Eds., R.S.H. Mah and W.D. Seider, AIChE, New York (1981).
18. Madsen, N.K., and R.F. Sincovec, "ALGORITHM 540: PDECOL, General Collocation Software for Partial Differential Equations [D3]," *ACM Trans. Math. Software*, **5**, p. 326 (1979).
19. Pirkle, Jr., J.C., and W.E. Schiesser, "Dynamic Simulation of Complex, Multistage Separation and Reactor Systems by a Modified DSS/2 Simulator," Paper No. 157d, AIChE Meeting, Miami (Nov. 2-7, 1986).
20. Pirkle, Jr., J.C., and W.E. Schiesser, "A Survey of PDE Software," *Proc. Summer Computer Simulation Conf.*, Simulation Councils, Inc., p. 89 (1986).